

An electron paramagnetic resonance study of the electron transport in heavily Si-doped high Al content $\text{Al}_x\text{Ga}_{1-x}\text{N}$

Cite as: AIP Advances 13, 125210 (2023); doi: 10.1063/5.0180912

Submitted: 12 October 2023 • Accepted: 14 November 2023 •

Published Online: 8 December 2023



View Online



Export Citation



CrossMark

M. E. Zvanut,^{1,a)} Jackson P. Hanle,¹ Subash Paudel,¹ Ryan Page,² Chandrashekhhar Savant,²
Yongjin Cho,³ H. Grace Xing,^{2,3,4} and Debdeep Jena^{2,3,4}

AFFILIATIONS

¹Department of Physics, University of Alabama at Birmingham, Birmingham, Alabama 35233, USA

²Department of Materials Science and Engineering, Cornell University, Ithaca, New York 14853, USA

³School of Electrical and Computer Engineering, Cornell University, Ithaca, New York 14853, USA

⁴Kavli Institute at Cornell for Nanoscale Science, Cornell University, Ithaca, New York 14853, USA

^{a)} Author to whom correspondence should be addressed: mezvanut@uab.edu

ABSTRACT

High Al mole fraction AlGaN is an ultrawide bandgap semiconductor with potential applications in power electronics and deep UV detectors. Although n-type material is achievable with Si-doping, the role of Si is controversial, particularly for $\text{Al}_x\text{Ga}_{1-x}\text{N}$ with $x > 0.8$. For this paper, AlGaN films were grown by plasma-assisted molecular beam epitaxy onto bulk AlN substrates and doped with 10^{18} – 10^{20} cm^{-3} Si. We examine electron transport in heavily Si-doped $\text{Al}_x\text{Ga}_{1-x}\text{N}$ with $x \geq 0.65$ using magnetic resonance, which allows us to probe the neutral donors directly rather than the free carriers and avoids complications due to electrical contacts. Transport was studied through the temperature-dependent linewidth of the electron paramagnetic resonance (EPR) signature for the neutral donor. Analysis shows evidence of hopping conductivity in the most lightly doped samples and impurity band formation in the most heavily doped ones. The EPR results, which are consistent with Hall measurements performed on the same samples, are promising for the development of highly conducting high Al content AlGaN.

© 2023 Author(s). All article content, except where otherwise noted, is licensed under a Creative Commons Attribution (CC BY) license (<http://creativecommons.org/licenses/by/4.0/>). <https://doi.org/10.1063/5.0180912>

I. INTRODUCTION

$\text{Al}_x\text{Ga}_{1-x}\text{N}$, where x ranges from 0 to 1, forms a family of semiconductors with applications including power electronics, optoelectronics, and photonics.^{1–3} One of the most significant features of this class of materials is the bandgap, especially the ultra-wide bandgap of AlN (6 eV) and high Al content $\text{Al}_x\text{Ga}_{1-x}\text{N}$ alloys (5–5.9 eV). In electronics, breakdown fields in excess of 10 MV/cm are thought to be achievable, and recently, Khachariya *et al.* exceeded this field in an $\text{Al}_{0.85}\text{Ga}_{0.15}\text{N}/\text{Al}_{0.6}\text{Ga}_{0.4}\text{N}$ high electron mobility transistor grown on an AlN substrate.^{2,4} For optical applications, the ultrawide bandgap will enable the LED industry to achieve devices with affordable deep ultraviolet spectral output. All devices based on these materials, though, require a predictable, controllable conductivity. For instance, ohmic contacts require a heavily doped low resistivity layer. Many advances have been made in the

fabrication of conducting n-type GaN devices by doping with Si; however, the addition of Al, particularly in excess of 70%, limits the efficiency of the Si n-type dopant.⁵ The Si donor level is 10–20 meV below the conduction band edge in GaN, but the level deepens with the addition of Al, reaching ~180 meV in AlN.^{6–9} Consequently, the number of free carriers at room temperature diminishes with increasing Al mole fraction. In addition, studies show that compensation by intrinsic defects, impurities like C or complexes, restricts the effectiveness of the Si dopant.^{10–12} However, recent work in which $\text{Al}_{0.65}\text{Ga}_{0.35}\text{N}$ was characterized by secondary ion mass spectrometry (SIMS), Hall measurements, and positron annihilation spectroscopy indicates that neither the common impurities nor the metal vacancy are responsible for compensation in their samples.¹³ Rather, some groups suggest that the Si dopant itself may introduce a form of self-compensation. Experiments suggest that in $\text{Al}_x\text{Ga}_{1-x}\text{N}$ ($x > 0.8$), Si forms a DX center, a shallow

donor with a negative correlation energy.^{14–17} On the other hand, theory predicts an Al concentration greater than 95% is needed for DX formation.¹⁸

To circumvent the limitations imposed by the donor level, some have explored the possibility of impurity band conduction, avoiding the need for excitation to the conduction band. Electrons are thought to hop among the dopants with activation on the order of meV depending on the type of dopant, its concentration, and the particular host. At a sufficiently high impurity concentration, several theories predict that the energy barrier for hopping approaches zero and temperature-independent electron transport is attained.¹⁹ This transition, referred to as the metal-to-insulator transition (MIT), is thought to occur at a critical concentration given by $N_c = \frac{0.25m^*}{\epsilon_r a^3}$. Here, N_c is the minimum concentration required for the transition, m^* is the relative effective mass of an electron, ϵ_r is the relative static dielectric constant, and a is the Bohr radius. Since the electron effective mass for AlN or $\text{Al}_x\text{Ga}_{1-x}\text{N}$ is not well established, predictions for the critical Si concentration vary. Nevertheless, several studies based on electrical measurements report impurity band conduction in various $\text{Al}_x\text{Ga}_{1-x}\text{N}$ alloys for Si concentration above $5 \times 10^{18} \text{ cm}^{-3}$,^{20,21} while others observe degenerate behavior at higher doping levels.^{22,23}

In this paper, we examine the issue of impurity band conduction from a different point of view—the temperature dependence of the spin relaxation time. Both hopping and impurity band conduction have been studied in n-type semiconductors via the temperature dependence of the spin relaxation time, but no one has addressed this issue in ultrawide bandgap high Al content AlGa_xN. Magnetic resonance studies typically monitor the linewidth of the neutral donor electron paramagnetic resonance (EPR) spectrum, which is inversely proportional to the spin relaxation time.²⁴ Hopping motion, impurity band formation, and the Mott transition have been investigated through analysis of the temperature-dependent EPR linewidth in semiconductors such as P-doped Si, Sb-doped Ge, n-type InSb and, more recently, Si-doped Ga₂O₃.^{25–27} Most pertinent to this paper are the studies of the donor resonance in unintentionally doped GaN and Si-doped GaN.^{28,29} In the following, we compare the magnetic resonance data of heavily Si-doped high Al content $\text{Al}_x\text{Ga}_{1-x}\text{N}$ with that of other semiconductor systems, in particular, GaN. The EPR results confirm the temperature-dependent Hall measurements indicating impurity band conduction and provide new information about transport at low temperature in the

lighter-doped samples where contact issues often compromise the electrical measurement. Finally, we note that for these high Al content AlGa_xN samples, the properties of the neutral donor reported here are the same as those for the donor in Si-doped GaN and require no consideration of a negative correlation or other types of self-compensation.

II. EXPERIMENTAL DETAILS

Samples were grown by plasma-assisted molecular beam epitaxy (MBE) on single crystal AlN substrates having low dislocation density ($<10^4 \text{ cm}^{-2}$) using standard effusion cells of Al, Ga, and Si. The native oxide on the substrate surface was removed prior to the growth using a combination of *ex situ* acid and *in situ* thermal treatment described in detail in Refs. 30 and 31. The substrate thermocouple temperatures for the growth were between 800 and 900 °C as calibrated by evaporation rates of Al and Ga.³⁰ For all samples, first, an AlN buffer layer of $\sim 1 \mu\text{m}$ was grown to isolate the AlGa_xN layer from substrate surface impurities and defects. Thereafter, an unintentionally doped (UID) AlGa_xN layer of 100–150 nm having the same composition as that of the doped AlGa_xN layer was grown. This UID AlGa_xN layer captures the Si present at the AlN surface and separates it from the top doped AlGa_xN layer.³² Finally, 10^{18} – 10^{20} cm^{-3} Si doped $\text{Al}_x\text{Ga}_{1-x}\text{N}$ layers of different compositions from $x = 0.65$ – 1 were grown. All samples were 150 nm doped $\text{Al}_x\text{Ga}_{1-x}\text{N}$ except for the sample with $x = 0.85$ and $5.6 \times 10^{19} \text{ cm}^{-3}$ Si, which was grown to 500 nm for more thorough EPR analysis.

Temperature-dependent Hall effect measurements were performed with a Lakeshore Hall system from 10 to 320 K using In contacts. Ohmic I–V curves were verified for most samples. Hall measurements were performed in standard van der Pauw arrangement using magnetic fields of -1 to $+1$ T. After the Hall measurements were completed, the samples were cut into $0.7 \times 0.25 \text{ cm}^2$ slices for EPR. EPR spectra were measured from 3.5 K to room temperature using an X-band spectrometer and liquid helium flow-through cryostat. Parameters such as microwave power and magnetic field modulation were chosen to avoid saturation effects while maintaining a reasonable signal-to-noise ratio. The EPR g-value, which is partially used to identify the spectra, is calculated as $g = \frac{hf}{\mu_B B}$, where h is Planck's constant, f is the microwave frequency, μ_B is the Bohr magneton, and B is the applied magnetic field.²⁴

TABLE I. Relevant properties of samples used in this paper.

	Al composition (at. %, XRD)	Si density (at./cm ³ , SIMS)	Layer thickness (nm, XRD)	4K spin density (cm ⁻³ , EPR)	Room temp carrier concentration (cm ⁻³ , Hall)	Effective activation energy (meV)
1 ^a	65	9.2×10^{18}	150	8×10^{17}		
2	78	2.67×10^{18}	150	$< 3 \times 10^{16}$	1.8×10^{16}	215.8
3	78	1.4×10^{20}	150	7×10^{17}	6.9×10^{19}	8.8
4	85	1.4×10^{20}	150	2×10^{17}	5.5×10^{19}	0.0
5	85	5.6×10^{19}	500	3×10^{17}	1.4×10^{19}	16.5
6 ^a	97.5	9.2×10^{18}	150	5×10^{16}		

^aThe carrier density and activation energy were unavailable for these samples.

Table I lists the significant features of the samples studied. X-ray diffraction reciprocal space mapping (XRD-RSM) of the AlGa_xN and AlN layers was carried out using a Bruker analytical x-ray diffractometer to confirm the fully strained condition of the AlGa_xN layer to underlying AlN in the 150 nm films (not shown). The Al composition and thickness of the AlGa_xN layer were determined from x-ray diffraction (XRD) symmetric (002) Ω -2 Θ scans, with simulation fitting using the fully strained condition as verified earlier with XRD-RSM. Time of flight-secondary ion mass spectrometry (ToF-SIMS) from Evans analytical group (EAG) was used to determine Si doping levels in the samples. The Si concentrations are estimated from an SIMS reference sample grown under the same conditions. The room temperature carrier density was determined from the temperature-dependent Hall data, and the effective activation energy was derived from the Arrhenius behavior of carrier density.²⁰ As will be discussed below, for the most heavily doped samples (3–5), the temperature dependence of the carrier concentration reflects impurity band conduction, so the effective activation energy reflects the energy barrier as the electron moves among the donors, not electron excitation to the conduction band edge. For EPR, the number of spins was calculated at each temperature by comparison to a standard, a heavily phosphorus-doped Si powder sample.²⁴ The concentration of spins, which was obtained by simply dividing by the sample volume, assumes a uniform distribution of defects.

III. RESULTS AND DISCUSSION

Figure 1 shows the EPR spectra of selected Al_xGa_{1-x}N samples measured at 4 K with the magnetic field parallel to the c-axis. Measurement of the AlN buffer grown on an AlN substrate produced no EPR signal, confirming that the resonances studied in this paper arise from the Al_xGa_{1-x}N film. The g-value calculated with the magnetic field parallel to the c-axis varies from 1.981

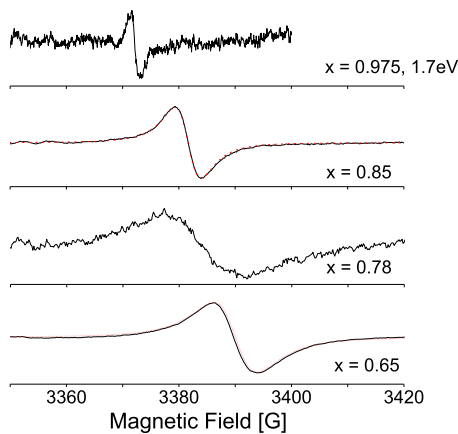


FIG. 1. EPR spectra of the neutral donor in Al_xGa_{1-x}N for Al mole fraction x listed in the figure: $x = 0.975$, sample 6; $x = 0.85$, sample 5; $x = 0.78$, sample 3; $x = 0.65$, sample 1. The $x = 0.975$ spectrum was taken during illumination with a 730 nm (1.7 eV) LED; the remaining were obtained without illumination. All spectra were measured at 4 K with the magnetic field parallel to the c-axis of the crystal. The dashed red lines are a Lorentzian fit.

to 1.990 as the Al mole fraction increases from 65% to 97.5% and does not change upon rotation in the c-plane. The increasing g-value as x increases, the narrowing of the line at nearly 100% Al, and nearly zero anisotropy is consistent with the signal reported by Bayerl *et al.* studying Al_xGa_{1-x}N with similar Al concentration and Si doping.³³ Thus, like in Ref. 33, we conclude that the EPR signal shown in Fig. 1 is due to a neutral donor. Although samples 1–5 were measured without intentional illumination, the EPR resonance of the sample with 97.5% Al was observed only after exposure to a 730 nm LED, consistent with reports of others.^{16,33} Because this sample required photoexcitation and the response was weak, we do not discuss the Al_{0.975}Ga_{0.025}N sample further. Using samples 1–5 described in Table I, we examine the temperature dependence of the EPR linewidth to gain insight into the possible transport mechanisms in heavily Si-doped high Al mole fraction Al_xGa_{1-x}N.

Samples 1 and 5 with the largest signal-to-noise ratio clearly exhibit a Lorentzian line shape over the temperature range of 3.5–200 K. See, for instance, the dashed lines in Fig. 1 for $x = 0.85$ and 0.65. The Lorentzian fit is typical of a shallow donor where the electron is only loosely bound to the impurity. Since the spectra in Fig. 1 establish all of the EPR signals as neutral donors, the spectra of the remaining samples were also analyzed as Lorentzian despite a somewhat diminished fit due to the low signal strength. Figure 2(a) shows the linewidth of the two most lightly doped samples (1, filled squares and 2, unfilled circles) over a range of temperatures, while Fig. 2(b) shows the same for the remaining samples. First, we point out that the temperature dependence of the linewidth follows the same trend as that previously reported for effective mass donors in different semiconductors including Si:P, Ge:As, as well as GaN:Si.^{25,26,28,29} Above 40 K (marked by the dashed line), the linewidth of all the samples broadens significantly; while at lower temperatures, the linewidth either decreases with increasing temperature [Fig. 2(a)] or increases slowly with temperature [Fig. 2(b)]. The trend above 40 K, which is typical of the donor resonance, is attributed to a decrease in the spin-lattice relaxation time caused by interaction with acoustic phonons.²⁸ We do not discuss this further here. Rather, the region of interest is $T < 40$ K, which is relevant to this paper.

For samples 1 and 2, the decrease in linewidth as the temperature is raised from 4 to 40 K is similar to that of donors in n-type GaN and is attributed to motional narrowing.^{28,29} The term refers to linewidth narrowing caused by the averaging of the nuclear hyperfine interaction as the electron moves among the local nuclear spins. The motion is often modeled as hopping. Maekawa and Kinoshita fit the temperature dependence of the linewidth in P-doped Si as

$$\Delta B \sim \tanh(E_0 / 2kT), \quad (1)$$

after consideration of the model of motional narrowing.²⁵ Here, ΔB is the linewidth, E_0 is the barrier between the filled (neutral donor) and unfilled (positively charged donor) sites, and k is Boltzmann's constant. The fit, the solid lines in Fig. 2(a), reveals an activation energy (E_0) of 1–3 meV, which is similar to hopping barriers measured electrically in many semiconductor systems.^{34–37} The temperature dependence of the linewidth in samples 3–5 is opposite to the trend observed in samples 1 and 2. Figure 2(b) shows

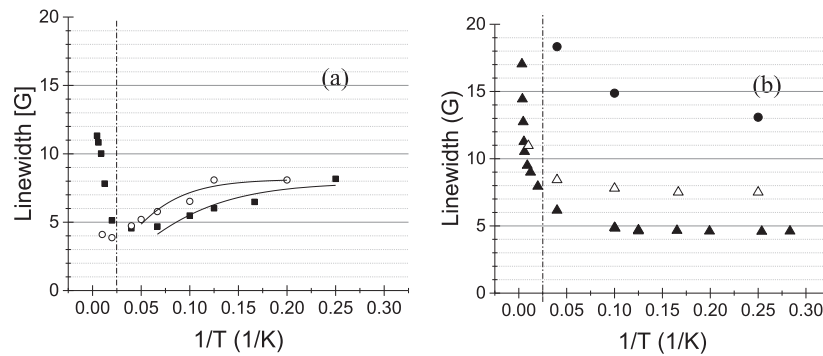


FIG. 2. (a) Lorentzian linewidth of low carrier concentration samples 1 (filled squares) and 2 (unfilled circles); the solid line represents a fit using Eq. (1). (b) Lorentzian linewidth of high carrier concentration samples 3 (filled circles), 4 (filled triangles), and 5 (unfilled triangles). Vertical dashed line indicates the onset of broadening due to acoustic phonons.

that these samples with room temperature carrier concentration of $1\text{--}7 \times 10^{19} \text{ cm}^{-3}$ exhibit an increasing linewidth as temperature increases from 4 to 40 K. The temperature dependence of the linewidth for effective mass donors in Si and GaN having the same carrier density is similar to that shown for samples 3–5.^{23,29} Wolos *et al.* point out that the linewidth increases with temperature as the free carrier density approaches the MIT. Thus, the EPR linewidth measurements for these samples are suggestive of impurity band conduction.

The temperature-dependent Hall measurements support the conclusions made above regarding the low-temperature transport mechanisms. Figure 3 shows the temperature dependence of the carrier density for samples 2 (unfilled circles), 3 (filled circles), and 4 (unfilled triangles) measured over a similar temperature range as the EPR measurements reported in Fig. 2. Sample 2, with the lowest carrier concentration, exhibits Arrhenius behavior at the higher temperatures (above 80 K), where activation to the conduction band begins. The effective activation energy reported in Table I is extracted from this high-temperature region.²² Below this region, the temperature dependence is dramatically different, showing minimal temperature dependence. We suggest that in this region where there is insufficient thermal energy to excite a

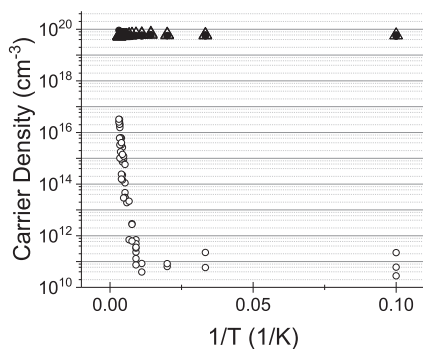


FIG. 3. Temperature-dependent Hall measurement of carrier density for samples 2 (unfilled circles), 3 (filled circles), and 4 (unfilled triangles).

measurable number of electrons to the conduction band, transport occurs by means of hopping, as indicated by the EPR data. Samples 3 and 4, with a carrier concentration of several orders of magnitude larger than sample 2, exhibit a nearly temperature-independent behavior from room temperature to 10 K, indicative of impurity band transport with sample 4 reaching the degenerate limit. Such data support the interpretation of the EPR linewidth data shown in Fig. 2(b). Thus, from the data of Figs. 2 and 3, the following description of transport in the Al-content AlGaN arises: the most lightly doped samples exhibit activated behavior, but near cryogenic temperatures hopping conductivity dominates; for carrier concentrations in excess of 5×10^{19} , only impurity band conduction is observed.

Comparison of the 4 K spin density and Si concentration also supports the transport picture described above. In all cases, the neutral donor density at 4 K is 2–3 orders of magnitude smaller than that of the Si. Typically, for a shallow donor in a lightly doped semiconductor, the EPR intensity reflects all the neutral donors in the sample when measured at 4 K. In the absence of compensation, the density of neutral donors, d^0 , is equal to the concentration of dopant impurities. This, clearly, is not the situation for the heavily doped samples used here. The apparent discrepancy, however, is consistent with the hopping/impurity band picture. Sample 2 is dominated by hopping conductivity at low temperature, so the difference between the Si and d^0 densities is at least partially due to compensation which is required for hopping transport.¹⁹ Transport in samples 3 and 5 is by means of an impurity band and approaches degenerate behavior in sample 4. As shown for donors in GaN with Si concentration similar to samples 3–5, the Mott–Hubbard model applies where conduction occurs in a D^- band and the neutral donor exists in the D^0 band.²⁹ The two-order of magnitude difference between d^0 and Si concentration is the same as that seen for similarly doped GaN.²⁹ Thus, unlike what may be expected from more lightly doped samples, the neutral donor density variation with Si concentration follows what is expected of a heavily doped nitride semiconductor exhibiting hopping and impurity band conduction.

Finally, a comment on whether the Si donor in these high Al content AlGaN samples is a DX center. As mentioned, the donor measured here behaves in the same manner as donors in other semiconductors, and nothing in the above analysis requires invoking

a negative electron correlation energy, which defines a DX center. Furthermore, both magnetic resonance and Hall measurements demonstrate that the Si donors in these samples exhibit impurity band conduction. Since the significant wave function overlap is required for impurity band conduction¹⁹ and the Si DX center is predicted to be a tightly bound defect,¹⁸ it would be surprising if the donors monitored here have DX character.

In summary, contactless measurements of the temperature-dependent EPR linewidth of heavily Si-doped high Al content $\text{Al}_x\text{Ga}_{1-x}\text{N}$ confirm that transport occurs via an impurity band in $\text{Al}_x\text{Ga}_{1-x}\text{N}$ ($1 > x \geq 0.78$) doped with $\sim 10^{20} \text{ cm}^{-3}$ Si and reveals hopping conductivity at low temperature in the lightly doped $\text{Al}_x\text{Ga}_{1-x}\text{N}$ ($x = 0.65, 0.78$). The results confirm that Si doping of AlGaN can yield large carrier densities and enable the development of highly conducting high Al content AlGaN.

ACKNOWLEDGMENTS

This work was supported as part of the Ultra-Materials for a Resilient Energy Grid, an Energy Frontier Research Center funded by the U.S. Department of Energy, Office of Science, Basic Energy Sciences under Award No. DE-SC0021230.

The EPR measurements and analysis were performed by the students at UAB; the sample growth, Hall measurements, and analysis were performed at Cornell University.

AUTHOR DECLARATIONS

Conflict of Interest

The authors have no conflicts to disclose.

Author Contributions

M. E. Zvanut: Conceptualization (lead); Formal analysis (supporting); Funding acquisition (lead); Project administration (lead); Resources (equal); Supervision (equal); Writing – original draft (lead); Writing – review & editing (lead). **Jackson P. Hanle:** Formal analysis (equal); Methodology (equal); Writing – original draft (supporting); Writing – review & editing (supporting). **Subash Paudel:** Formal analysis (supporting). **Ryan Page:** Formal analysis (supporting). **Chandrashekhhar Savant:** Formal analysis (supporting). **Yongjin Cho:** Formal analysis (supporting). **H. Grace Xing:** Conceptualization (supporting); Formal analysis (supporting); Funding acquisition (equal); Methodology (equal); Resources (equal); Writing – review & editing (supporting). **Debdeep Jena:** Funding acquisition (equal); Methodology (supporting); Resources (equal).

DATA AVAILABILITY

The data that support the findings of this study are available from the corresponding author upon reasonable request.

REFERENCES

¹B. Sarkar, P. Reddy, F. Kaess, B. B. Haidet, J. Tweedie, S. Mita, R. Kirste, E. Kohn, R. Collazo, and Z. Sitar, “Material considerations for the development of III-nitride power devices,” *ECS Trans.* **80**, 29 (2017).

²R. J. Kaplar, A. A. Allerman, A. M. Armstrong, M. H. Crawford, J. R. Dickerson, A. J. Fischer, A. G. Baca, and E. A. Douglas, “Review—Ultra-wide-bandgap AlGaIn power electronic devices,” *ECS J. Solid State Sci. Technol.* **6**, Q3061 (2017).

³M. Kneissl, T. Y. Seong, J. Han, and H. Amano, “The emergence and prospects of deep-ultraviolet light-emitting diode technologies,” *Nat. Photonics* **13**, 233 (2019).

⁴D. Khachariya, S. Mita, P. Reddy, S. Dangi, J. H. Dycus, P. Bagheri, M. H. Breckenridge, R. Sengupta, S. Rathkanthiwar, R. Kirste, E. Kohn, Z. Sitar, R. Collazo, and S. Pavlidis, “Record >10 MV/cm mesa breakdown fields in $\text{Al}_{0.85}\text{Ga}_{0.15}\text{N}/\text{Al}_{0.6}\text{Ga}_{0.4}\text{N}$ high electron mobility transistors on native AlN substrates,” *Appl. Phys. Lett.* **120**, 172106 (2022).

⁵R. Collazo, S. Mita, J. Xie, A. Rice, J. Tweedie, R. Dalmau, and Z. Sitar, “Progress on n-type doping of AlGaIn alloys on AlN single crystal substrates for UV optoelectronic applications,” *Phys. Status Solidi C* **8**, 2031 (2011).

⁶W. Gotz, N. M. Johnson, C. Chen, H. Liu, C. Kuo, and W. Imler, “Activation energies of Si donors in GaN,” *Appl. Phys. Lett.* **68**, 3144 (1996).

⁷P. Hacke, A. Maekawa, N. Koide, K. H. Kazumasa Hiramatsu, and N. S. Nobuhiko Sawaki, “Characterization of the shallow and deep levels in Si doped GaN grown by metal-organic vapor phase epitaxy,” *Jpn. J. Appl. Phys.* **33**, 6443 (1994).

⁸Y. Taniyasu, M. Kasu, and N. Kobayashi, “Intentional control of n-type conduction for Si-doped AlN and $\text{Al}_x\text{Ga}_{1-x}\text{N}$ ($0.42 \geq x > 1$),” *Appl. Phys. Lett.* **81**, 1255 (2002).

⁹M. L. Nakarmi, K. H. Kim, K. Zhu, J. Y. Lin, and H. X. Jiang, “Transport properties of highly conductive n-type Al-rich $\text{Al}_x\text{Ga}_{1-x}\text{N}$ ($x \geq 0.7$),” *Appl. Phys. Lett.* **85**, 3769 (2004).

¹⁰P. Reddy, Q. Guo, T. James, S. Washiyama, F. Kaess, S. Mita, M. H. Breckenridge *et al.*, “Improving the conductivity limits in Si doped Al rich AlGaIn,” in *2018 IEEE Research and Applications of Photonics in Defense Conference (RAPID)* (IEEE, 2018), pp. 1–4.

¹¹I. Bryan, Z. Bryan, S. Washiyama, P. Reddy, B. Gaddy, B. Sarkar, M. H. Breckenridge, Q. Guo, M. Bobeja, J. Tweedie, S. Mita, D. Irving, R. Collazo, and Z. Sitar, “Doping and compensation in Al-rich AlGaIn grown on single crystal AlN and sapphire by MOCVD,” *Appl. Phys. Lett.* **112**, 062102 (2018).

¹²B. Liu, F. Xu, J. Wang, J. Lang, L. Wang, X. Fang, X. Yang, X. Kang, X. Wang, Z. Qin, W. Ge, and B. Shen, “Correlation between electrical properties and growth dynamics for Si-doped Al-rich AlGaIn grown by metal-organic chemical vapor deposition,” *Micro Nanostruct.* **163**, 107141 (2022).

¹³A. S. Almogbel, C. J. Zollner, B. K. Saifaddin, M. Iza, J. Wang, Y. Yao, M. Wang, H. Foronda, I. Prozheev, F. Tuomisto, A. Albadri, S. Nakamura, S. P. DenBaars, and J. S. Speck, “Growth of highly conductive Al-rich AlGaIn:Si with low group-III vacancy concentration,” *AIP Adv.* **11**, 095119 (2021).

¹⁴M. S. Brandt, R. Zeisel, S. T. B. Gönnerwein, M. W. Bayerl, and M. Stutzmann, “DX behaviour of Si donors in AlGaIn alloys,” *Phys. Status Solidi B* **235**, 13 (2003).

¹⁵F. Mehnke, X. T. Trinh, H. Pingel, T. Wernicke, E. Janzen, N. T. Son, and M. Kneissl, “Electronic properties of Si-doped $\text{Al}_x\text{Ga}_{1-x}\text{N}$ with aluminum mole fractions above 80,” *J. Appl. Phys.* **120**, 145702 (2016), and references therein.

¹⁶R. Zeisel, M. W. Bayerl, S. T. B. Gönnerwein, R. Dimitrov, O. Ambacher, M. S. Brandt, and M. Stutzmann, “DX-behavior of Si in AlN,” *Phys. Rev. B* **61**, R16283 (2000).

¹⁷A. Kakanakova-Georgieva, S.-L. Sahonta, D. Nilsson, X. T. Trinh, N. T. Son, E. Janzén, and C. J. Humphreys, “n-Type conductivity bound by the growth temperature: The case of $\text{Al}_{0.72}\text{Ga}_{0.28}\text{N}$ highly doped by silicon,” *J. Mater. Chem. C* **4**, 8291–8296 (2016).

¹⁸L. Gordon, J. L. Lyons, A. Janotti, and C. G. Van de Walle, “Hybrid functional calculations of DX centers in AlN and GaN,” *Phys. Rev. B* **89**, 085204 (2014).

¹⁹N. F. Mott and W. D. Twose, “The theory of impurity conduction,” *Adv. Phys.* **10**(38), 107 (1961).

²⁰K. Zhu, M. L. Nakarmi, K. H. Kim, J. Y. Lin, and H. X. Jiang, “Silicon doping dependence of highly conductive n-type $\text{Al}_{0.7}\text{Ga}_{0.3}\text{N}$,” *Appl. Phys. Lett.* **85**, 4669 (2004).

- ²¹P. Pampili, D. V. Dinh, V. Z. Zubialevich, and P. J. Parbrook, "Significant contribution from impurity-band transport to the room temperature conductivity of silicon-doped AlGaN," *J. Phys. D: Appl. Phys.* **51**, 06LT01 (2018).
- ²²S. Bharadwaj, S. M. Islam, K. Nomoto, V. Protasenko, A. Chaney, H. (Grace) Xing, and D. Jena, "Bandgap narrowing and Mott transition in Si-doped Al_{0.7}Ga_{0.3}N," *Appl. Phys. Lett.* **114**, 113501 (2019).
- ²³K. Kataoka, T. Narita, K. Nagata, H. Makino, and Y. Saito, "Electronic degeneracy conduction in highly Si-doped Al_{0.6}Ga_{0.4}N layers based on the carrier compensation effect," *Appl. Phys. Lett.* **117**, 262103 (2020).
- ²⁴J. A. Weil, J. R. Bolton, and J. E. Wertz, *Electron Paramagnetic Resonance* (John Wiley & Sons, Inc, New York, 1994).
- ²⁵S. Maekawa and N. Kinoshita, "Electron spin resonance in phosphorus doped silicon at low temperatures," *J. Phys. Soc. Jpn.* **20**, 1447 (1965).
- ²⁶E. M. Gershenzon, N. M. Pevin, and M. S. Fogelson, "Some features of ESR and spin-lattice relaxation of electrons in Ge and InSb with different donor concentrations," *Phys. Status Solidi B* **38**, 865 (1970).
- ²⁷H. J. von Bardeleben and J. L. Cantin, "Unusual conduction mechanism of n-type β -Ga₂O₃: A shallow donor electron paramagnetic resonance analysis," *J. Appl. Phys.* **128**, 125702 (2020).
- ²⁸W. E. Carlos, J. A. Freitas, Jr., M. A. Khan, D. T. Olson, and J. N. Kuznia, "Electron-spin-resonance studies of donors in wurtzite GaN," *Phys. Rev. B* **48**, 879 (1993).
- ²⁹A. Wolos, Z. Wilamowski, M. Piersa, W. Strupinski, B. Lucznik, I. Grzegory, and S. Porowski, "Properties of metal-insulator transition and electron spin relaxation in GaN:Si," *Phys. Rev. B* **83**, 165206 (2011).
- ³⁰K. Lee, Y. Cho, L. J. Schowalter, M. Toita, H. G. Xing, and D. Jena, *Appl. Phys. Lett.* **116**, 262102 (2020).
- ³¹Y. Cho, C. S. Chang, K. Lee, M. Gong, K. Nomoto, M. Toita, L. J. Schowalter, D. A. Muller, D. Jena, and H. G. Xing, *Appl. Phys. Lett.* **116**, 172106 (2020).
- ³²K. Lee, R. Page, V. Protasenko, L. J. Schowalter, M. Toita, H. G. Xing, and D. Jena, *Appl. Phys. Lett.* **118**, 092101 (2021).
- ³³M. W. Bayerl, M. S. Brandt, T. Graf, O. Ambacher, J. A. Majewski, M. Stutzmann, D. J. As, and K. Lischka, "g values of effective mass donors in Al_xGa_{1-x}N alloys," *Phys. Rev. B* **63**, 165204 (2001).
- ³⁴A. Avdonin, P. Skupiński, and K. Graszka, "Experimental investigation of the typical activation energy and distance of hopping electron transport in ZnO," *Physica B* **562**, 94 (2019).
- ³⁵W. C. Mitchel, A. O. Ewaeaye, S. R. Smith, and M. D. Roth, "Hopping conduction in heavily doped bulk n-type SiC," *J. Electron. Mater.* **26**, 113 (1997).
- ³⁶D. C. Look, D. C. Reynolds, W. Kim, Ó. Aktas, A. Botchkarev, A. Salvador, and H. Morkoc, "Deep-center hopping conduction in GaN," *J. Appl. Phys.* **80**, 2960 (1996).
- ³⁷D. C. Look, "Electrical transport properties of III-nitrides," *Mater. Sci. Eng. B* **50**, 50 (1997).